

# Development of Optically Transparent Cyclic Olefin Photoresist Binder Resins

Larry F. Rhodes<sup>\*a</sup>, Chun Chang<sup>a</sup>, Cheryl Burns<sup>a</sup>, Dennis A. Barnes<sup>a</sup>, Brian Bennett<sup>a</sup>, Larry Seger<sup>a</sup>, Xiaoming Wu<sup>a</sup>, Andy Sobek<sup>a</sup>, Mike Mishak<sup>a</sup>, Craig Peterson<sup>a</sup>, Leah Langsdorf<sup>a</sup>, Hideo Hada<sup>b</sup>, Hiroaki Shimizu<sup>b</sup>, Kazuhito Sasaki<sup>b</sup>

<sup>a</sup>Promerus LLC, 9921 Brecksville Rd, Brecksville OH 44141 USA

<sup>b</sup>Tokyo Ohka Kogyo Co. Ltd., 1590, Tabata, Samukawa-machi, Koza-gun, Kanagawa-ken, 253-0114 Japan

## ABSTRACT

Of all candidate 193 nm photoresist binder resins, transition metal catalyzed vinyl addition cyclic olefin (i.e., norbornene) polymers (PCO) hold the promise of high transparency and excellent etch resistance. In order to access lower molecular weight polymers, which are typically used in photoresists,  $\alpha$ -olefin chain transfer agents (CTAs) are used in synthesizing vinyl addition poly(norbornenes). For example, HFANB ( $\alpha,\alpha$ -bis(trifluoromethyl)bicyclo[2.2.1]hept-5-ene-2-ethanol) homopolymers (p(HFANB)) with molecular weights ( $M_n$ ) less than 5000 have been synthesized using such chain transfer agents. However, the optical density (OD) at 193 nm of these materials was found to rise as their molecular weights decreased consistent with a polymer end group effect. Extensive NMR and MS analysis of these polymers revealed that olefinic end groups derived from the chain transfer agent were responsible for the deleterious rise in OD. Chemical modification of these end groups by epoxidation, hydrogenation, hydrosilation, etc. lowers the OD of the polymer by removing the olefinic chromophore, however, it does require a second synthetic step. Thus a new class of non-olefinic chain transfer agents has been developed at Promerus that allow for excellent control of vinyl addition cyclic olefin polymer molecular weight and low optical density without the need of a post-polymerization chemical modification. Low molecular weight homopolymers of HFANB have been synthesized using these chain transfer agents that exhibit ODs  $\leq 0.07$  absorbance units per micron. This molecular weight control technology has been applied to both positive tone and negative tone vinyl addition cyclic olefin binder resins. Lithographic and etch performance of positive tone photoresists based on these binder resins will be presented.

**Keywords:** Cyclic olefin, norbornene, photoresist, transparency, 193 nm

## 1. INTRODUCTION

An important characteristic of photoresist films that impacts lithographic performance is dissolution behavior in developer. This characteristic is profoundly affected by molecular weight and molecular weight distribution of the binder resin.<sup>1</sup> For example, high molecular weight poly(*p*-hydroxystyrene) (PHS) dissolves more slowly in aqueous base than its low molecular weight counterparts. Therefore control of molecular weight and molecular weight distribution of binder resins is critical.

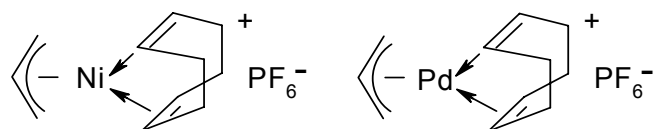
Another important characteristic of the photoresist film that enhances lithographic performance is transparency at the imaging wavelength. In moving from 248 nm to 193 nm imaging radiation, the semiconductor industry has auditioned several new polymeric materials as binder resins based on their transparency at 193 nm: methacrylates, norbornene/maleic anhydride copolymers (COMA-type polymers), norbornene/maleic anhydride/acrylate polymers (hybrid polymers) and vinyl addition norbornene polymers. Unique among these polymers, vinyl addition norbornene polymers hold the promise of both transparency as well as excellent etch resistance.<sup>2</sup>

Vinyl addition norbornene polymers are made using transition metal catalysts. Janiak and Lassahn have reviewed the literature regarding these metal catalysts up to 2001.<sup>3</sup> Late transition metal catalysts, in particular palladium, allow the polymerization of norbornene monomers possessing pendant functionalities such as acid labile, hydrophilic, and base

\*[larry.rhodes@promerus.com](mailto:larry.rhodes@promerus.com); phone 440-922-1443; fax 216-803-2319, [www.promerus.com](http://www.promerus.com).

soluble groups. These pendant groups are used to tailor the properties of photoresist binder resins. Their incorporation is made possible by the wide functional tolerance of palladium.<sup>4</sup>

The structures of two early generation cationic norbornene polymerization catalysts are shown below. Control of the molecular weight of vinyl addition poly(norbornenes) using the nickel catalyst was readily achieved using  $\alpha$ -olefin and ethylene CTAs. However, palladium was less susceptible to chain transfer using  $\alpha$ -olefins.<sup>4</sup>

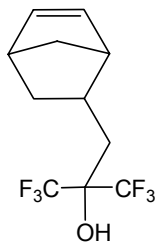


Recognizing this limitation, Promerus subsequently developed a new generation of high activity norbornene vinyl addition palladium catalysts that are more responsive to  $\alpha$ -olefin CTAs.<sup>5</sup>

Recently, several publications have appeared that discuss the incorporation of the bis-trifluorocarbonol substituted norbornene, HFANB, into photoresist binder resins.<sup>6,7</sup> HFANB is of interest since it imparts aqueous base solubility to polymers while its preponderance of carbon-fluorine bonds increases the polymer's optical transparency, especially at short wavelengths. In particular, vinyl addition copolymers of HFANB and the t-butylester of 5-norbornene carboxylic acid were found to have utility as binder resins in 157 nm photoresist formulations.<sup>7</sup> Terpolymers containing HFANB were capable of printing sub 100 nm features at 193 nm.<sup>8</sup>

Given the importance of HFANB in the photoresist industry, we explored the homopolymerization of HFANB catalyzed by our new generation of palladium catalysts using  $\alpha$ -olefin CTAs to control molecular weight. During the course of our study, we found that while low molecular weight polymers can be accessed using these catalyst systems, the optical density of these polymers was quite high.

The OD can be lowered by post-polymerization chemical modification, requiring an extra synthetic step. To avoid the need for such an extra synthetic step, Promerus has developed new non-olefinic CTAs that allow both allow control of molecular weight and result in a low OD polymer. This technology has been applied to PCO binder resins for chemically amplified, positive tone photoresists. Lithographic and etch properties of these photoresists developed by Tokyo Ohka Kogyo Co. (TOK) are discussed.



HFANB

## 2. EXPERIMENTAL

### 2.1 Materials.

The synthesis of HFANB has been described previously.<sup>7b</sup> HFANB homopolymers were synthesized and epoxidized according to procedures disclosed in the patent literature.<sup>9</sup>

### 2.2 Instrumental analysis.

The  $^1\text{H}$  NMR spectra were recorded on a Bruker AV-500 NMR spectrometer. Chemical shifts were referenced using internal solvent resonances and were reported relative to tetramethylsilane or were referenced to internal tetramethylsilane.

Polymer molecular weights were determined by GPC according to the following procedure. Approximately 50-60 mg of polymer was dissolved in 20 mL of tetrahydrofuran containing 250 mg BHT. The solution was filtered through a 0.2-micron Teflon® disposable syringe filter and then injected into the chromatograph. The chromatographic conditions were: Mobile phase, THF stabilized with 250 ppm BHT; Pump, Waters 515 pump at 1.0 mL/min; Autosampler, Micromeritics Model 708; Sample, ~0.25% concentration, 100  $\mu$ L injection volume; Column, 2 Phenomenex Linear (2) columns, plus 1 Phenomenex 50A column, 5 micron, in series; Column Oven, Waters, 40°C; Detector, Waters 2410 Refractive Index at 40°C. The data for analysis was acquired using Waters' Millennium LC/GPC network software, version 3.2. Calibration was obtained using EasiCal polystyrene standards from Polymer Laboratories. The calibration range was  $7.5 \times 10^6$ –162 Dalton.

MALDI-TOF MS (Matrix-Assisted Laser Desorption Ionization-Time of Flight Mass Spectrometry) were recorded using a Bruker Reflex III instrument in the linear mode. Spectra were obtained in the negative ion mode. Sinapinic acid matrix was prepared as a saturated solution in 1:1 acetonitrile/water. The polymer samples were dissolved in THF (0.1 g/mL). Equal volumes of the matrix and sample solutions were mixed prior to syringe deposition on a stainless steel MALDI plate.

### 2.3 Optical density determination.

The optical density (OD) of the polymers were determined by the following method. A 15 weight percent solution of the desired polymer was prepared using propylene glycol methylether acetate (PGMEA). The solution was dispensed onto a 1-inch quartz wafer and spun at 500 rpm for 10 sec and 2000 rpm for 60 sec. The wafers were then baked for 60 sec at 130 °C on a hotplate and the optical absorbance measured at 193 nm using a Cary 400 Scan UV-Vis spectrophotometer. The film thickness was then measured using a TENCOR profilometer after the films were scored. Optical density of the film was calculated by dividing the absorbance by the thickness (in microns).

### 2.4 Lithography.

The resist was spin coated onto a wafer having 77 nm thick layer of organic bottom antireflective coating (BARC) ARC-29 (Shipley) to a thickness of 225 nm. The coated wafers were soft-baked at 95 °C for 60 seconds and exposed at 193 nm using a Nikon NSR-302 (NA 0.60) or NSR-306 (NA 0.78) through a 6% half tone mask. After a post-exposure bake, also at 95 °C for 60 seconds, the resist was developed in NMD-3 2.38% TMAH (Tokyo Ohka Kogyo Co.) for 30 seconds with an ACT-8 system. The critical dimensions (CD) were measured with a Hitachi S-9220 scanning electron microscope (SEM). Cross-sectional resist profiles were observed by using a Hitachi S-4700 SEM.

### 2.5 Etch.

Etching rates of unexposed areas were measured after using a CF<sub>4</sub>/CHF<sub>3</sub>/He mixed gas etch process with a parallel-plate-type system (TCE-7811X, Tokyo Ohka Kogyo Co.). Etching conditions: gas pressure was 300 mTorr, flow rates of CF<sub>4</sub>, CHF<sub>3</sub> and He were 40 sccm, 40 sccm, and 120 sccm, respectively, and acceleration power was 700W. Surface roughness was evaluated with a Hitachi S-4700 SEM.

## 3. RESULTS AND DISCUSSION

### 3.1 Synthesis of p(HFANB) using new generation Pd catalysts and ethylene CTA.

Recently, Promerus revealed a new generation of palladium catalysts for cyclic olefin polymerization that are defined by high activity and good response to  $\alpha$ -olefin and ethylene CTAs.<sup>5</sup> Earlier generations of Promerus palladium catalysts were described as containing weakly coordinating ligands such as 1,4-cyclooctadiene or even solvent.<sup>4,10</sup> A necessary component in these new palladium catalysts is the relatively stronger electron donating Group 15 ligand. The presence of this type of ligand apparently allows for a more stable palladium complex that can, in turn, be heated during polymerization without suffering from decomposition. The new generation catalysts still require a weakly coordinating anion to balance the charge and an easily accessible coordination site to allow close approach of the cyclic olefin to the metal center. As such, a generic formula for such catalysts can be constructed as shown below. R is a hydrocarbyl group, L' a group 15 ligand (e.g., a phosphine), S is a neutral two-electron donor ligand that can be readily replaced by monomer, and WCA is a weakly coordinating anion. Using this type of catalyst, p(HFANB) can be made in excellent yield with relatively low catalyst loadings.

## [R'Pd(L')<sub>x</sub>(S)]<sup>+</sup> WCA

The response of p(HFANB) molecular weight to increasing ethylene concentration using the new generation palladium polymerization catalyst system is shown in Figure 1. The molecular weights ( $M_n$ ) of the isolated p(HFANB) ranged from 25,000 (at lower concentration ethylene) to less than 5000 (at higher ethylene concentration). A similar trend is found when 1-hexene is used as a CTA. Clearly, low molecular weight cyclic olefin addition polymers are accessible using this catalyst system. Contrast this to results obtained for p(HFANB) with early generation palladium catalysts in which, "...addition of 1-hexene did not significantly reduce the molecular weight of the Pd(II) catalyzed polymers..."<sup>7b</sup>

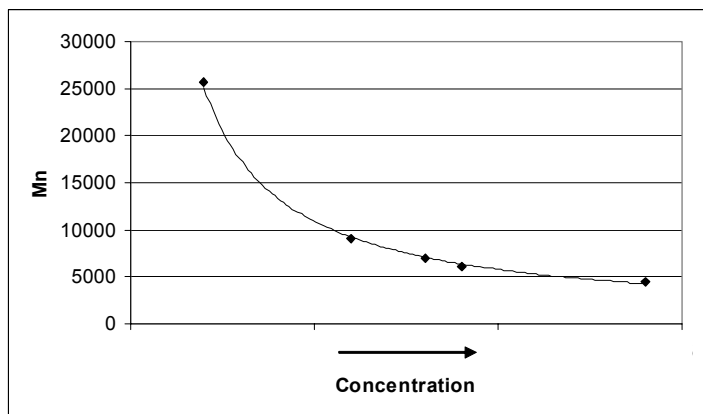


**Figure 1.** Plot of p(HFANB)  $M_n$  vs. concentration of ethylene.

### 3.1 NMR and MALDI-TOF MS analysis of p(HFANB).

The structure of p(HFANB) made using ethylene as a CTA was investigated by both <sup>1</sup>H NMR and MALDI-TOF MS techniques. A representative <sup>1</sup>H NMR spectrum in CDCl<sub>3</sub> of a relatively low molecular weight homopolymer of HFANB ( $M_n = 3260$ ) made using ethylene as a chain transfer agent is shown in Figure 2. The peaks in the 0.5-2.6 ppm region of the spectrum account for protons on the aliphatic carbons 1-8 (see structure below). The hydroxylic proton 9 is assigned to the broad chemical shift appearing between 2.6 and 3.3 ppm. This assignment is confirmed by addition of D<sub>2</sub>O to the NMR tube which results in a shift of the hydroxylic hydrogen resonance to ~4.8 ppm by H/D exchange. In Figure 2, two small, broad resonances are observed in the olefinic region of the spectrum at 5.00 ppm and 5.86 ppm. These two resonances are assigned to the vinyl terminus (protons on carbons 10 and 11 in the structure below) of the polymer chain derived from chain transfer to ethylene.

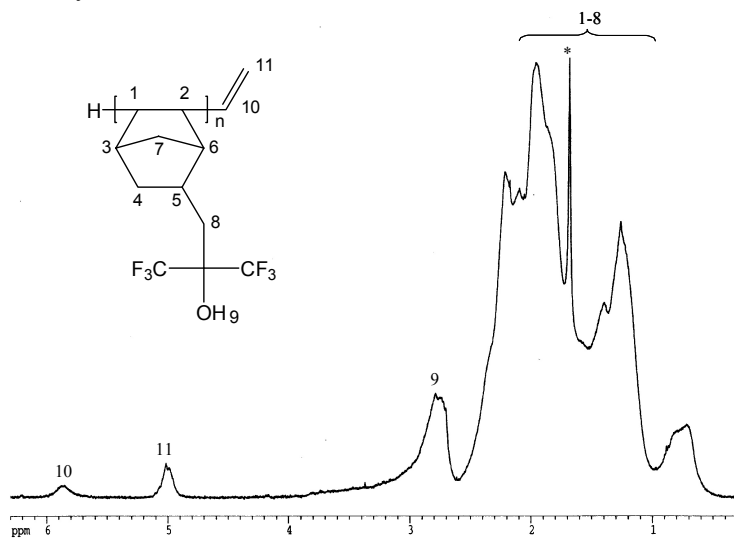


**Figure 2.** <sup>1</sup>H NMR spectrum of p(HFANB) made using ethylene as CTA (\* = water).

A MALDI-TOF MS (negative ion mode) trace of the same HFANB homopolymer is presented in Figure 3. Only one significant polymer series is observed and it is consistent with vinyl and hydrogen terminated poly(HFANB). Since in the negative ion mode, loss of  $H^+$  from the polymer chain occurs, an HFANB polymer chain with a degree of polymerization of 10, for example, and a vinyl and hydrogen end group would exhibit a molecular ion of 2767 as is observed in the mass spectrum. A much less intense polymer series is observed (marked with \* in Figure 3) which is consistent with the loss of  $CF_3H$  (70 Daltons) from the polymer chain.

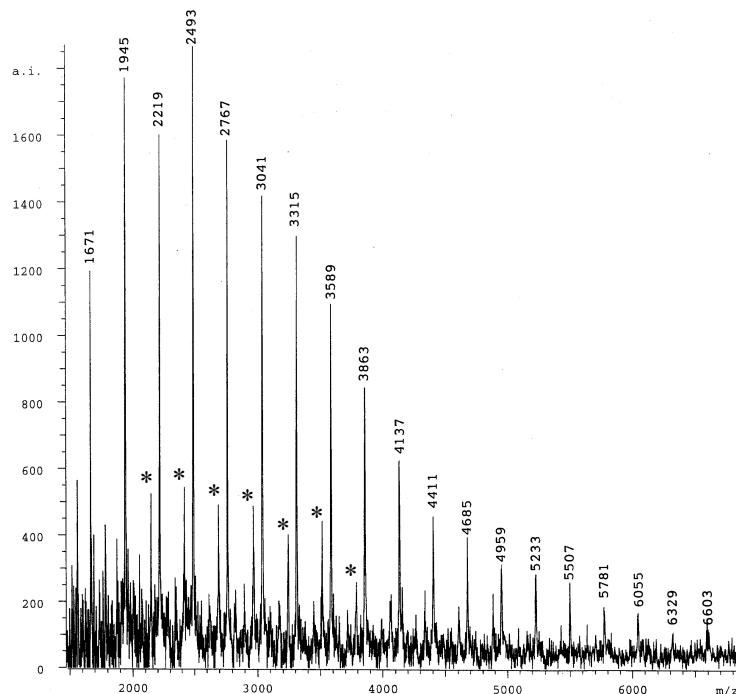


**Figure 3.** MALDI-TOF MS of p(HFANB) made using ethylene as CTA (\* = loss of  $CF_3H$ ).

The mechanism for formation of the vinyl-terminated poly(norbornene) has been documented in previous publications<sup>4, 5b</sup> and will not be discussed here.

### 3.2 Optical density of vinyl-terminated p(HFANB).

The optical density (OD) of different molecular weight homopolymers of HFANB made using both ethylene and 1-hexene (in toluene and anisole solvents) as chain transfer agents was measured at 193 nm. The results of these optical density measurements (in absorbance units/micron) are presented as a function of  $M_n$  in Figure 4.

An inverse relationship exists between OD and molecular weight for the homopolymer of HFANB is observed; that is to say, as the molecular weight decreases, the OD increases. At approximately 8000  $M_n$ , the OD is about 0.20 absorbance units/micron, while at lower molecular weight, about 3000  $M_n$ , the OD increases to about 0.35 absorbance units/micron. At very high molecular weight ( $M_n = 53600$ ), the OD is extremely low, 0.07 absorbance units/micron.

This observed trend suggests that polymer end groups are a major influence on OD since as the molecular weight decreases, the relative concentration of polymer end groups increases. If end groups absorb at 193 nm, then an increase in OD would be expected. The presence of olefinic end groups in homopolymers of HFANB have been established using both  $^1H$  NMR and MALDI-TOF MS techniques. Ethylene exhibits a  $\pi$  to  $\pi^*$  transition at 165 nm. Substitution of ethylene results in a bathochromic shift of this absorbance. Tetraalkyl substituted alkenes exhibit a  $\lambda_{max}$  below 200 nm, but the band widths are sufficiently broad such that significant absorption can occur above 200 nm.<sup>11</sup> Thus, it appears reasonable that an increased concentration of absorbing olefinic end groups is responsible for the increase in OD at lower molecular weights shown in Figure 4. At high molecular weight the end group concentrations are small and their contribution to absorbance should vanish. This explains the ~0.07 OD value for p(HFANB) with an  $M_n = 53600$ . This

suggests that the inherent absorption of p(HFANB) is exceedingly small at 193 nm and is consistent with the observation that end groups play a role in photoresist sensitivity and transparency in other polymer systems.<sup>12</sup>

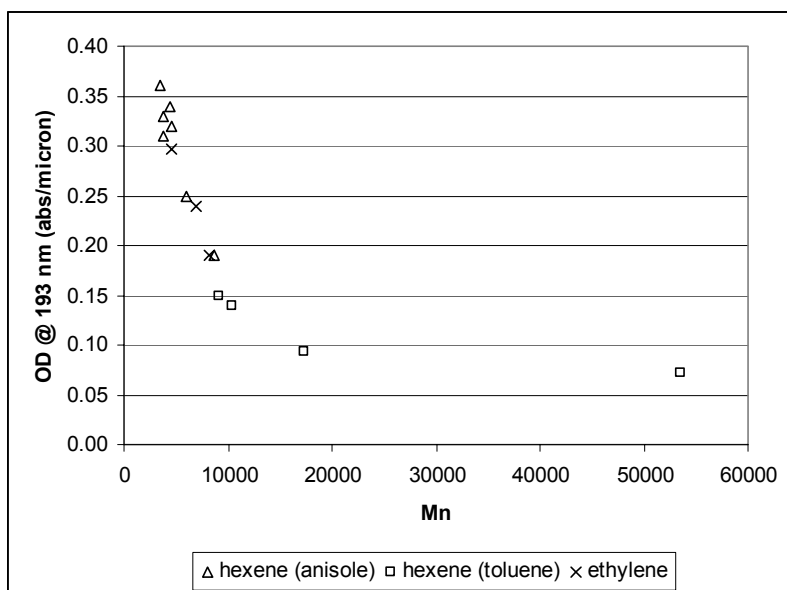


**Figure 4.** Plot of OD (193 nm) for p(HFANB) made using 1-hexene (in toluene and anisole) and ethylene as CTA.

### 3.3 End group modification of vinyl-terminated p(HFANB).

The behavior observed in Figure 4 is at odds with the desire to employ low molecular weight *and* low OD vinyl addition norbornene polymers as binder resins made using olefin chain transfer agents. Extremely low OD is only attained at high molecular weight. Thus a method of reducing the optical absorbance of such end groups that is independent of molecular weight was sought. One possible avenue of investigation would be to chemically transform the polymer end groups into less absorbing species.

The method of end group modification that was explored to reduce the optical density of olefin-terminated polymers was epoxidation using peroxyacetic acid. This method was particularly attractive since it did not require further addition of metal catalysts to the binder resin, unlike hydrogenation and hydrosilation, which were also found to be effective modification methods.<sup>9b</sup> The vinyl-terminated p(HFANB) was treated with a mixture of acetic acid and hydrogen peroxide at elevated temperatures. After workup, the peroxyacetic acid treated, vinyl-terminated polymer was analyzed by <sup>1</sup>H NMR spectroscopy. Essentially all the vinyl resonances were consumed. Addition of D<sub>2</sub>O to the NMR tube shifted the polymer hydroxylic protons down-field, revealing a broad resonance at about 2.95 ppm which is assigned to an epoxy end group hydrogen. In the case of the hexenyl-terminated polymer, no olefinic residues were observed by <sup>1</sup>H NMR spectrometry. The mass spectrum (MALDI-TOF) of the peroxyacetic acid treated, vinyl-terminated homopolymer is presented in Figure 5. It is consistent with the formation of an epoxy terminated homopolymer. For p(HFANB) with a degree of polymerization of 10 and hydrogen and epoxy end groups, the molecular ion (M-H)<sup>-</sup> would be 2783 as is observed in Figure 5. Analogous results were obtained for peroxyacetic acid treated p(HFANB) made using 1-hexene as the CTA.

The optical densities at 193 nm of four such peroxyacetic acid treated homopolymers of HFANB (three hexenyl-terminated and one vinyl-terminated) with different molecular weights were determined. As shown in Figure 6, (see circled data points), all four polymers, with  $M_n$ s from about 4000 to 10000, exhibited ODs between 0.06 to 0.08 absorbance units/micron, substantially lower than that observed for the untreated olefin-terminated homopolymers.

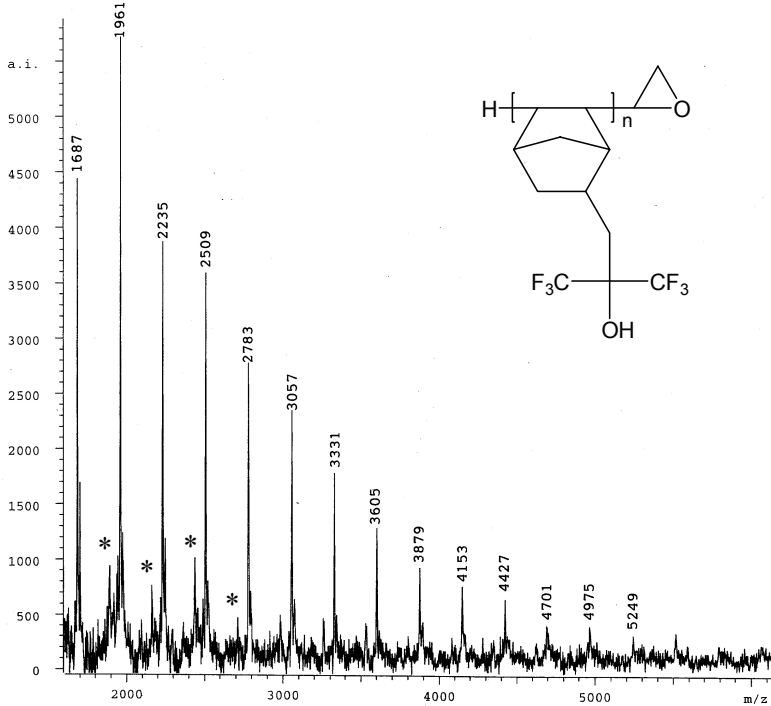


**Figure 5.** MALDI-TOF MS of epoxy-terminated p(HFANB) (\* = loss of  $\text{CF}_3\text{H}$ ).

Thus, modification of the olefinic end groups of the p(HFANB) by epoxidation results in substantially lower OD films. Clearly, the resulting epoxy end groups are less absorbing at 193 nm than the double bond containing end groups they are formed from. Aliphatics are relatively transparent at 193 nm and epoxides exhibit a  $\lambda_{\text{max}}$  at  $\sim 170$  nm.<sup>11</sup> In addition, the optical density response of the peroxyacetic acid treated polymers is invariant to changes in molecular weight. Thus, by transformation of the olefin end group chromophores in p(HFANB) to less absorbing species, low optical density poly(norbornene)s can be accessed irrespective of their molecular weight. Therefore, end group modification has been demonstrated as a valid method for optical density reduction for poly(norbornene) binder resins that could be used in photoresists.

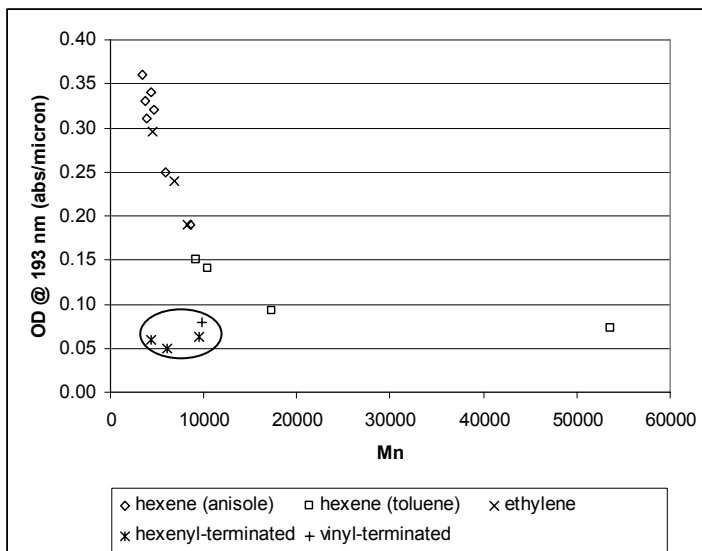


**Figure 6.** Plot of OD vs.  $M_n$  for p(HFANB) treated with peroxyacetic acid (circled) overlaid on Figure 4.

### 3.4 Development of non-olefinic chain transfer agents.

Despite the ability to control poly(norbornene) molecular weight using  $\alpha$ -olefin CTAs and the ability to reduce the optical density of the polymers formed by post-polymerization epoxidation, the two-step process is not an attractive approach for binder resin development. Thus, at Promerus, new, non-olefinic chain transfer agents that would both control molecular weight and deliver polymers with low OD values independent of molecular weight without the need for post-polymerization processing were sought and discovered. The molecular weight response of p(HFANB) formed using these new CTAs and our new generation of palladium catalysts is shown in Figure 7.

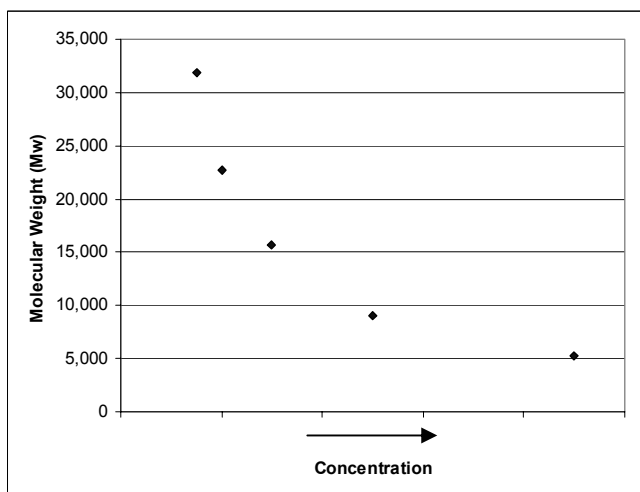


**Figure 7.** Plot of p(HFANB) molecular weight ( $M_w$ ) vs. concentration of non olefinic CTA.

Note that low molecular weight polymers similar to that found for ethylene in Figure 1, are accessible using this new family of CTAs but that unlike such polymers from Figure 1, the p(HFANB)s formed using non-olefinic CTAs have extremely low OD. A comparison of OD data observed for both olefin-terminated and peroxyacetic acid treated p(HFANB)s is shown in Figure 8. The ODs of p(HFANB) made using the non-olefinic CTAs are at least comparable to that observed for peroxyacetic acid treated p(HFANB) (ODs as low as 0.05 were recorded). Also the ODs are essentially equal to that observed for p(HFANB) at extremely high molecular weight where end group effects should be negligible.

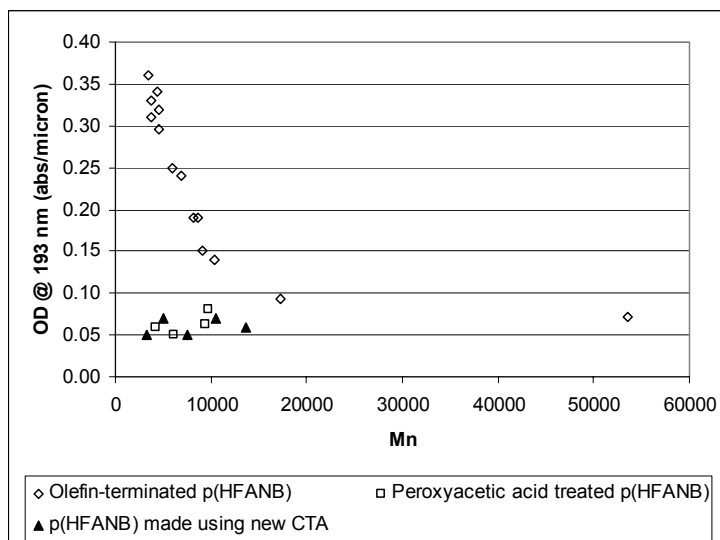


**Figure 8.** Comparison of OD vs.  $M_n$  for olefin-terminated and peroxyacetic acid treated p(HFANB) to p(HFANB) made using non-olefinic CTAs.

Clearly accessing low OD polymers independent of molecular weight without the need of post-polymerization modification was a breakthrough discovery and was immediately employed in the production of polymer compositions containing acid labile pendant groups. Such polymers were formulated into positive tone resists at TOK.

### **3.5 Lithographic performance.**

While PCO has an excellent advantage with regard to etch resistance, early generation PCOs exhibited higher than desirable absorbance at 193 nm. In general, it is well known that higher absorbance at the exposure wavelength of the photoresist polymer will affect pattern profile. However, with the new polymerization process developed by Promerus, that problem has been resolved. Thus, PCOs now offer wider applicability as photoresist polymers.

In order to investigate the effect of OD on lithographic performance, PCOs of different optical densities were evaluated. See Figure 9. While the higher OD formulation exhibited tapered patterns, the lower OD formulation showed improved imaging. Thus, OD (transparency) improvement contributed to better pattern profiles.

TOK optimized the photoresist formulation and process using these lower OD PCOs. As a result, TOK succeeded in confirming good lithographic performance for Contact Hole applications. See Figure 10. For 100 nm Contact Holes, good hole shape with equal or better focus margin compared to conventional photoresist formulations (i.e., methacrylate) was achieved. Thus the new generation low OD PCO-based photoresists improved pattern profile and its lithographic performance is proved to be competitive to that of conventional type photoresist.

### **3.6 Etch performance.**

PCO is widely known to exhibit “good etch performance”. Figure 11 shows blanket etching resistance test results. Here, we have used an acrylate type polymer that has been widely employed for ArF Photoresist formulation as a comparison. In the acrylate type formulation, it is known that the higher acrylate ratio in the polymer, the slower the etch rate and the better the surface roughness. While a 100% acrylate formulation photoresist does have good etch resistance, it, unfortunately, suffers from poor lithographic performance. As a result, actual ArF formulations, either hybrid type with a mixture of acrylate and methacrylate monomers or 100% methacrylates are being used commercially. However, PCO-based photoresists have equal etch-rate and surface roughness performance to those of 100% acrylate formulation while maintaining good litho performance. Figure 12 shows actual patterned etching test results. Compared with conventional photoresist, PCO offers improved pattern shape (i. e., more circular) after etching. Also, photoresist film retention after etching is 10-20% greater than that of conventional type photoresist. See Figures 11 and 13.

From these results, it was confirmed that new generation PCOs exhibit excellent etch resistance with improved lithographic resolution. Thus, PCO is very promising candidate as an ArF photoresist binder resin.

## **4. CONCLUSIONS**

In this contribution, we have shown that the new generation of high activity palladium catalysts for norbornene vinyl addition polymerization developed at Promerus are responsive to olefinic chain transfer agents. In this regard molecular weights of less than 5000 ( $M_n$ ) can be achieved for p(HFANB). However, these polymers exhibit an inverse relationship between molecular weight and optical density at 193 nm due to the presence of the absorbing olefinic end groups. While the optical density can be decreased by post-polymerization modification, this requires two synthetic steps. This was overcome by discovery of non-olefinic chain transfer agents that create controlled molecular weight polymers with low optical densities that are independent of molecular weight. Positive tone polymer compositions were synthesized using these chain transfer agents. These polymers were formulated and their lithographic and etch characteristics were evaluated at TOK in contact hole applications. Lithographic performance of these polymers was found to be equivalent to methacrylates. The contact hole profile of PCOs was better than methacrylates after etch and 10-20% better than methacrylates in terms of film thickness retention. The latter result becomes increasingly important as feature sizes shrink and film thicknesses are reduced concomitantly.

Future work will concentrate on polymer compositions specifically tailored to line/space and trench applications.

## ACKNOWLEDGMENTS

Dr. R. Lattimer recorded the MALDI-TOF MS and Dr. G. Benedikt recorded the NMR spectra reported herein. The authors thank A. Uno and J. McDaniel for their support of this work.

## REFERENCES

1. (a) Tsiartas, P. C.; Simpson, L. L.; Qin, A.; Willson, C. G.; Allen, R. D.; Krukonis, V. J.; Gallagher-Wetmore, P. M. *Proc. SPIE-Int. Soc. Opt. Eng.* **1995**, 2438, 261. (b) Thompson, L. F.; Willson, C. G.; Bowden, M. J. *Introduction to Microlithography* 2<sup>nd</sup> Edition; American Chemical Society: Washington, DC, 1994; p. 197.
2. (a) Goodall, B. L.; Jayaraman, S.; Shick, R. A.; Rhodes, L. F. US 6136499, 2000. (b) Allen, R. D.; Sooriyakumaran, R.; Opitz, J.; Wallraff, G. M.; Breyta, G.; Dipietro, R. A.; Hofer, D. C.; Okoroanyanwu, U.; Willson, C. G. *J. Photopolym. Sci. Tech.* **1996**, 9(3), 465. (c) Okoroanyanwu, U.; Shimokawa, T.; Byers, J.; Willson, C. G. *Chem. Mater.* **1998**, 10, 3319. (d) Okoroanyanwu, U.; Shimokawa, T.; Byers, J.; Willson, C. G. *J. Mol. Catal. A: Chem.* **1998**, 133, 93. (e) Wallow, T.; Brock, P.; DiPietro, R.; Allen, R.; Opitz, J.; Sooriyakumaran, R.; Hofer, D.; Meute, J.; Byers, J.; Rich, G.; McCallum, M.; Schuetze, S.; Jayaraman, S.; Hullihen, K.; Vicari, R.; Rhodes, L. F.; Goodall, B.; Shick, R. *Proc. SPIE-Int. Soc. Opt. Eng.* **1998**, 3333, 92. (f) Varanasi, P. R.; Maniscalco, J.; Mewherter, A. M.; Lawson, M. C.; Jordhamo, G.; Allen, R. D.; Opitz, J.; Ito, H.; Wallow, T. I.; Hofer, D.; Langsdorf, L.; Jayaraman, S.; Vicari, R. *Proc. SPIE-Int. Soc. Opt. Eng.* **1999**, 3678, 51. (g) Varanasi, P. Rao; Mewherter, A. M.; Lawson, M. C.; Jordhamo, G.; Allen, R.; Opitz, J.; Ito, H.; Wallow, T.; Hofer, D. *J. Photopolym. Sci. Technol.* **1999**, 12(3), 493.
3. Janiak, C.; Lassahn, P. G. *J. Mol. Catal.* **2001**, 166, 193.
4. Goodall, B. L. in *Late Transition Metal Polymerization Catalysis* Rieger, B; Saunders Baugh, L.; Kacker, S.; Striegler, S., Ed.; Wiley-VCH: Weinheim, Germany, 2003, p 101.
5. (a) Lipian, J.-H.; Rhodes, L. F.; Goodall, B. L.; Bell, A.; Mimna, R. A.; Fondran, J. C.; Jayaraman, S.; Hennis, A. D.; Elia, C. N.; Polley, J. D.; Sen, A. US Patent 6455650, 2002. (b) Lipian, J.; Mimna, R. A.; Fondran, J. C.; Yandulov, D.; Goodall, B. L.; Rhodes, L. F.; Shick, R. A.; Huffman, J. C. *Macromolecules* **2002**, 35, 8969. (c) Hennis, A.; Polley, J.; Sen, A.; Yandulov, D.; Lipian, J.; Benedikt, G.; Rhodes, L. F.; Huffman, J. *Organometallics*, **2001**, 20, 2802.
6. (a) Ito, H.; Seehof, N.; Sato, R.; Nakayama, T.; Ueda, M. in *Micro- and Nanopatterning Polymers*; H. Ito, E. Reichmanis, O. Nalamasu, T. Ueno, Eds.; ACS Symposium Series 706, American Chemical Society: Washington, DC, 1998, 208. (b) Ito, H.; Wallraff, G. M.; Fender, N.; Brock, P. J.; Larson, C. E.; Truong, H. D.; Breyta, G.; Miller, D. C.; Sherwood, M. H.; Allen, R. D. *J. Photopolymer Sci. Tech.* **2001**, 14(4), 583. (c) Padmanaban, M.; Alemy, E.; Bae, J.-B.; Kim, W.-K.; Kudo, T.; Masuda, S.; Rahman, D.; Sakamuri, R.; Dammel, R.; Jung, J.-C.; Lee, S.-K.; Shin, K.-S. *J. Photopolymer Sci. Tech.* **2001**, 14(4), 631. (d) Ito, H.; Truong, H. D.; Okazaki, M.; Miller, D. C.; Fender, N.; Brock, P. J.; Wallraff, G. M.; Larson, C. E.; Allen, R. D. *J. Photopolymer Sci. Tech.* **2002**, 15(4), 591. (e) Toriumi, M.; Ishikawa, T.; Kodani, T.; Koh, M.; Moriya, T.; Araki, T.; Aoyama, H.; Yamashita, T.; Yamazaki, T.; Furukawa, T.; Itani, T. *J. Photopolymer Sci. Tech.* **2003**, 16(4), 607.
7. (a) Chiba, T.; Hung, R. J.; Yamada, S.; Trinque, B.; Yamachika, M.; Brodsky, C.; Patterson, K.; Van der Heyden, A.; Jamison, A.; Lin, S.-H.; Somervell, M.; Byers, J.; Conley, W.; Willson, C. G. *J. Photopolymer Sci. Tech.* **2000**, 13(4), 657. (b) Tran, H. V.; Hung, R. J.; Chiba, T.; Yamada, S.; Mrozek, T.; Hsieh, Y.-T.; Chambers, C. R.; Osborn, B. P.; Trinque, B. C.; Pinnow, M. J.; MacDonald, S. A.; Willson, C. G.; Sanders, D. P.; Connor, E. F.; Grubbs, R. H.; Conley, W. *Macromolecules* **2002**, 35, 6539. (c) Dammel, R. R.; Sakamuri, R.; Kudo, T.; Romano, A.; Rhodes, L.; Vicari, R.; Hacker, C.; Conley, W.; Miller, D. *J. Photopolymer Sci. Tech.* **2001**, 14(4), 603. (d) Tran, H. V.; Hung, R. J.; Chiba, T.; Yamada, S.; Mrozek, T.; Hsieh, Y.-T.; Chambers, C. R.; Osborn, B. P.; Trinque, B. C.; Pinnow, M. J.; Sanders, D. P.; Connor, E. F.; Grubbs, R. H.; Conley, W.; MacDonald, S. A.; Willson, C. G. *J. Photopolymer Sci. Tech.* **2001**, 14(4), 669. (e) Houlihan, F.; Romano, A.; Rentkiewicz, D.; Sakamuri, R.; Dammel, R. R.; Conley, W.; Rich, G.; Miller, D.; Rhodes, L.; McDaniel, J.; Chang, C. *J. Photopolymer Sci. Tech.* **2003**, 16(4), 581.
8. Li, W.; Varanasi, P. R.; Lawson, M. C.; Kwong, R. W.; Chen, K.-J.; Ito, H.; Truang, H.; Allen, R.; Yamamoto, M.; Kobayashi, E.; Slezak, M. *Proc. SPIE-Int. Soc. Opt. Eng.* **2003**, 5039, 61
9. (a) Rhodes, L. F.; Barnes, D. A.; Bell, A.; Bennett, B.; Chang, C.; Lipian, J.-H.; Wu, X., US 2004229157, 2004. (b) Rhodes, L. F.; Vicari, R.; Langsdorf, L. J.; Sobek, A. A.; Boyd, E. P.; Bennett, B., US 20030176853, 2003. (c) see 5a.

- 
- 10 (a) Mathew, J. P.; Reinmuth, A.; Melia, J.; Swords, N.; Risse, W. *Macromolecules* **1996**, *29*, 2755.  
11. Pasto, D. J ; Johnson, C. R. *Laboratory Text for Organic Chemistry* Prentice-Hall, Englewood Cliffs, NJ, 1979, p. 110-111.  
12. (a) Ito, H.; England, W. P.; Lundmark, S. B. *Proc. SPIE-Int. Soc. Opt. Eng.* **1992**, *1672*, 2. (b) Momose, H.; Wakabayashi, S.; Fujiwara, T.; Ichimura, K.; Nakauchi, J. *Proc. SPIE-Int. Soc. Opt. Eng.* **2001**, *4345*, 695. (c) Ito, H.; Miller, D. C.; Sherwood, M. *J. Photopolymer Sci. Tech.* **2000**, *13*(4), 559. (d) Barclay, G. G.; Hawker, C. J.; Ito, H.; Orellana, A.; Mallenfant, P. R. L.; Sinta, R. F. *Macromolecules*, **1998**, *31*, 1024.
- 
- 

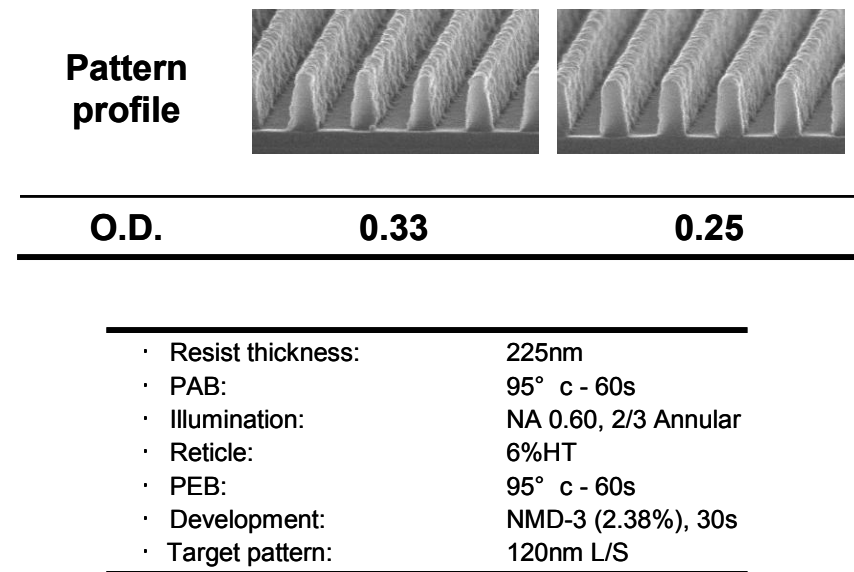


**Figure 9.** Effect of optical density on pattern profile.

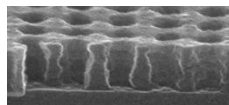
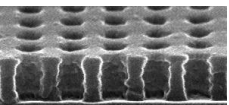
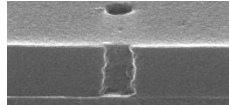
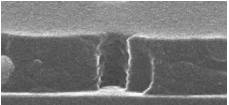
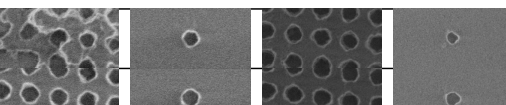
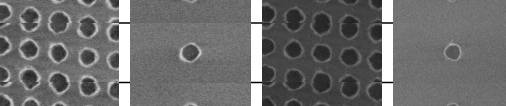
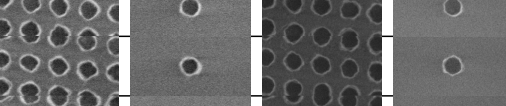
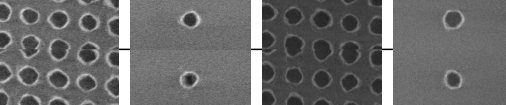
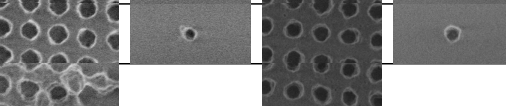
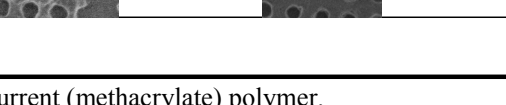
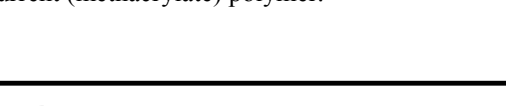
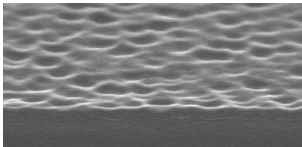
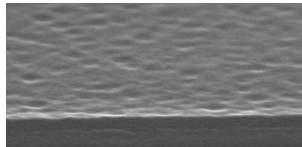
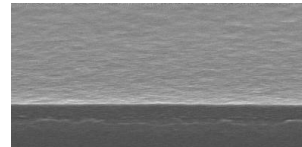
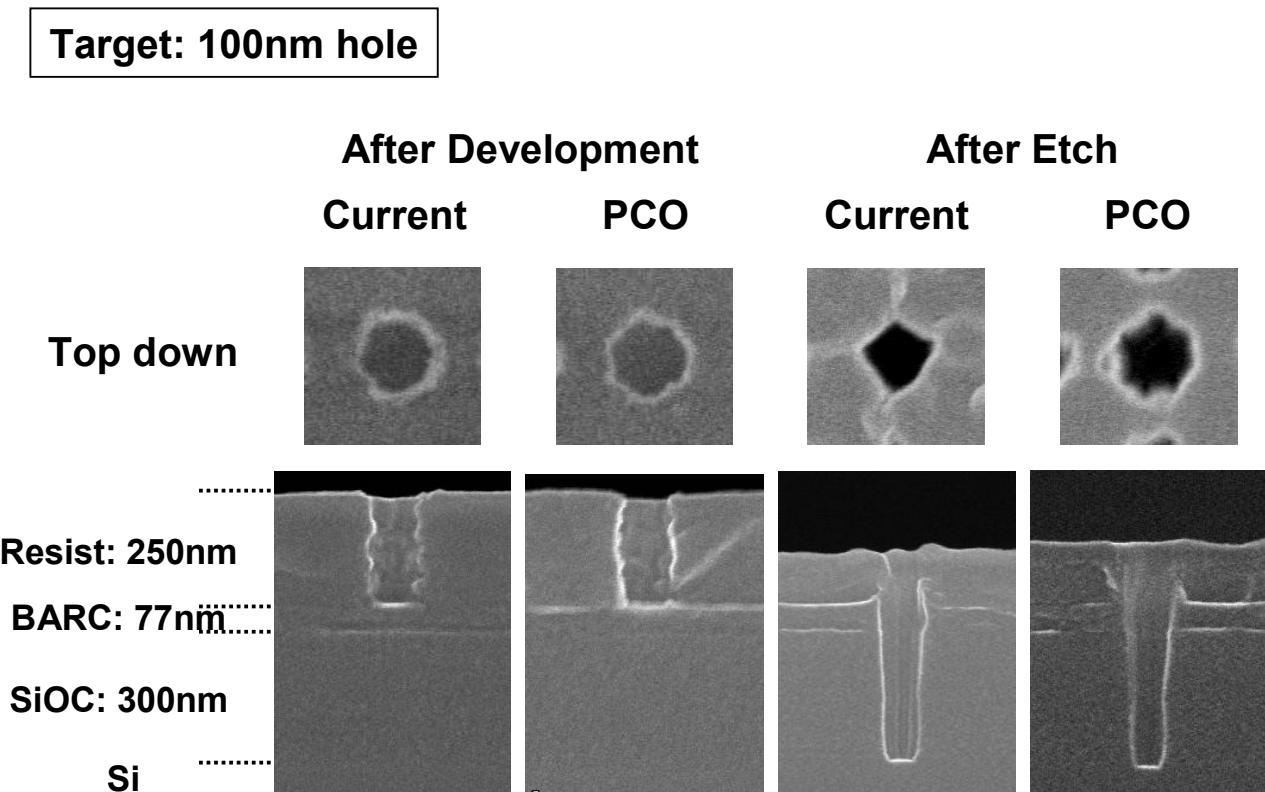
<u>Cross section</u>		<u>Focus latitude</u>	
Current	PCO	Current	PCO
Bake	<b>100/110</b>	<b>95/95</b>	
Dense			
Iso			
		250nm	
		200nm	
		150nm	
		100nm	
		50nm	
		Center	
		-50nm	
		-100nm	
		-150nm	
		-200nm	
		-250nm	
<b>Target pattern</b>			
Iso	100nm CH (mask 140nm, pitch 1540nm)		
Dense	100nm CH (mask 140nm, pitch 200nm)		

Figure 10. Resist performance of PCO compared to current (methacrylate) polymer.

Methacrylate Acryl ratio : 0	Hybrid Acryl ratio : 60	Acrylate Acryl ratio : 100	PCO
			
<b>Rate : 55.4nm/min</b>	<b>Rate : 52.1nm/min</b>	<b>Rate : 49.5nm/min</b>	<b>Rate : 50.0nm/min</b>
<ul style="list-style-type: none"> <li>Substrate: Bare Si</li> <li>Resist thickness: 400 nm</li> <li>Gas(ml/min): CF4:40, CHF3:40, He:120</li> <li>Pressure: 300mtoer</li> <li>ESC: +/-700w</li> <li>Back He: 30ml/15torr</li> <li>Pole temp.: 25c</li> <li>Stage temp.: 20c</li> </ul>			

**Figure 11.** Comparison of etching rate and surface roughness for methacrylate, hybrid, acrylate and PCO polymer.



**Figure 12.** Comparison of pattern profiles after development and etching.

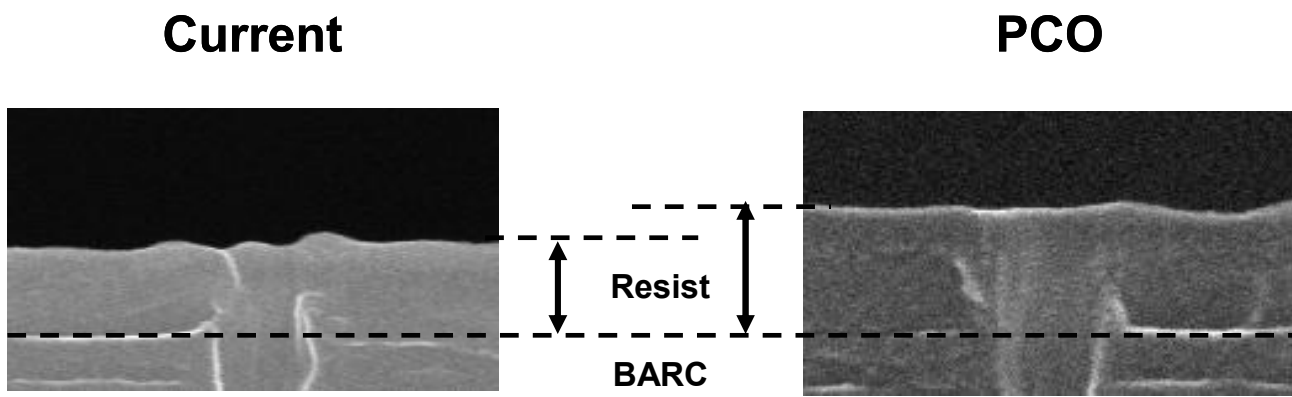


**Figure 13.** Comparison of resist thickness after etching for current (methacrylate) and PCO polymer.